5536 *J. Med. Chem.* **2010,** *53,* 5536–5548
DOI: 10.1021/jm100194a

Journal of Medicinal Chemistry
Article

Development and Characterization of New Inhibitors of the Human and Mouse Hematopoietic Prostaglandin D_2 Synthases

Angelika N. Christ,[†,§] Larisa Labzin,[†,§] Gregory T. Bourne,[†] Hirotada Fukunishi,[‡] Jane E. Weber,[†] Matthew J. Sweet,[†] Mark L. Smythe,[†] and Jack U. Flanagan*,[†]

[†]*Institute for Molecular Bioscience, The University of Queensland, Queensland, 4072, Australia, and* [‡]*Research Center, Shiseido Company Ltd., 2-2-1 Hayabuchi, Tsuzuki-ku, Yokohama 224-8558, Japan.* [§]*These authors contributed equally to this work.*

Received February 12, 2010

The hematopoietic prostaglandin D_2 synthase has a proinflammatory effect in a range of diseases, including allergic asthma, where its product prostaglandin D_2 (PGD_2) has a role in regulating many of the hallmark disease characteristics. Here we describe the development and characterization of a novel series of hematopoietic prostaglandin D_2 synthase inhibitors with potency similar to that of known inhibitors. Compounds *N*-benzhydryl-5-(3-hydroxyphenyl)thiophene-2-carboxamide (compound **8**) and *N*-(1-amino-1-oxo-3-phenylpropan-2-yl)-6-(thiophen-2-yl)nicotinamide (compound **34**) demonstrated low micromolar potency in the inhibition of the purified enzyme, while only **34** reduced Toll-like receptor (TLR) inducible PGD_2 production in both mouse primary bone marrow-derived macrophages and the human megakaryocytic cell line MEG-01S. Importantly, **34** demonstrated a greater selectivity for inhibition of PGD_2 synthesis versus other eicosanoids that lie downstream of PGH_2 (PGE_2 and markers of prostacyclin (6-keto $PGF_{1\alpha}$) and thromboxane (TXB_2)) when compared to the known inhibitors HQL-79 (compound **1**) and 2-phenyl-5-(1*H*-pyrazol-3-yl)thiazole (compound **2**). Compound **34** therefore represents a selective hematopoietic prostaglandin D_2 synthase inhibitor.

Introduction

Prostaglandins (PG[a]) are a family of structurally related eicosanoids that have important roles in homeostasis but also contribute to the pathology of numerous inflammatory diseases.[1] The cyclooxygenase enzymes catalyze the conversion of arachidonic acid to PGH_2, which is converted to other prostanoid species including PGD_2, PGE_2, $PGF_{2\alpha}$, prostacyclin (PGI_2), and thromboxane (TX) A_2 by the action of specific synthases. Each prostanoid has different biological activities;[2] for example, during inflammation PGE_2 is a major mediator of pain, fever, and swelling,[3] whereas PGD_2 is a major proinflammatory mediator of the allergic response.[4] PGI_2 and TXA_2 largely have opposing biological activities; PGI_2 prevents platelet aggregation and promotes dilation of blood vessels, while TXA_2 promotes platelet aggregation and blood vessel constriction. Consequently, cyclooxygenase inhibition affects a number of biological processes with adverse effects[5] such as the gastric toxicity and the more seldom cardiovascular complications associated with prostacyclin loss.[6] Targeting individual synthases downstream of cyclooxygenase represents a strategy to avoid these complications.

PGD_2 is active in both the central nervous system and peripheral tissues, with roles in body temperature regulation, sleep–wake regulation, relaxation of smooth muscle, tactile pain response, bronchoconstriction, and inflammation. In mouse models of asthma and allergic disease, the prostanoid has a substantial proinflammatory effect, regulating many hallmark characteristics including eosinophilia, airways hyperreactivity, mucus production, and Th2 cytokine levels.[7−9] Moreover, inhibition of PGD_2 synthesis and PGD_2 signaling blockade had a suppressive effect on neuroinflammation in mouse models of Krabbe's disease.[10] In contrast to these proinflammatory effects, PGD_2 and its cyclopentenone PG derivatives also have anti-inflammatory properties, with functions in inflammation resolution.[11]

Isomerization of the cyclooxygenase product PGH_2 to PGD_2 is performed by two genetically distinct PGD_2 synthase (PGDS) enzymes, brain-type PGDS and hematopoietic PGDS (see refs 12 and 13 for reviews). The former is a member of the lipocalin superfamily, termed L-PGDS, while the latter, termed H-PGDS, is the only vertebrate member of the glutathione transferase (GST) σ class and requires glutathione (GSH) to perform the isomerization reaction. Other members of the σ class include GSTs from squid[14] and chicken,[15] a cephalopod lens *S*-crystallin[16], and a PGD_2 synthase from the parasite *Onchocerca volvulus*.[17] The divergence in biochemical activity and likely in vivo function exhibited by the σ class GSTs is also reflected in the differences in tissue distribution.

*To whom correspondence should be addressed. Current address: Auckland Cancer Society Research Centre, University of Auckland, Grafton, Auckland 1032, New Zealand. Phone: +64 9 373 7599, extension 86155. Fax: +64 9 373 7571. E-mail: j.flanagan@auckland.ac.nz.

[a]Abbreviations: PG, prostaglandin; H-PGDS, hematopoietic prostaglandin D2 synthase; L-PGDS, lipocalin-type prostaglandin D2 synthase; GST, glutathione transferase; GSH, glutathione; H-site, hydrophobic site; CDNB, 1-chloro-2,4-dinitrobenzene; DMSO, dimethyl sulfoxide; TLR, Toll-like receptor; MeCN, acetonitrile; TFA, trifluoroacetic acid; DCM, dichloromethane; EtOAc, ethyl acetate; DIEA, diisopropylethylamine; MeOH, methanol; EtOH, ethanol; DMF, *N*,*N*-dimethylformamide; HBTU, *O*-benzotriazol-1-yl-*N*,*N*,*N*′,*N*′-tetramethyluronium hexafluorophosphate; PyBrOP, benzotriazole-1-yloxytripyrrolidinophosphonium hexafluorophosphate; DIEA, *N*,*N*-diisopropylethylamine; $Pd(PPh_3)_4$, tetrakis(triphenylphosphine)palladium(0); CsF, cesium fluoride; CuI, copper(I) iodide; $MgSO_4$, magnesium sulfate.

 Published on Web 07/20/2010

The highest levels of expression for the mammalian H-PGDS include the spleen and bone marrow,[18] while the chicken GST isoform is expressed in the liver, kidney, and intestine,[18] and the squid GST transcript was found predominantly in the digestive gland.[16] Moreover, as mammalian L-PGDS expression appears to be mostly restricted to the central nervous system, testis, and heart,[13] PGD_2 synthesis in peripheral tissues is likely to be through the H-PGDS GSH dependent mechanism.

The GSTs are a family of detoxifying enzymes that can catalyze the conjugation of glutathione (GSH) to many compounds bearing electrophilic functional groups.[19] The σ class enzymes exist as cytosolic homodimers and have a similar tertiary structure and active site topology, despite low sequence identity, compared to the other classes.[20] The monomer can be divided into two domains, with the active site existing at the domain interface. The mixed α/β N-terminal domain contains the GSH binding site (G site), while the all helical C-terminal domain contributes to the PGH_2 binding site/hydrophobic substrate binding site (H site).[21,22] A key feature of the conjugation reaction catalyzed by GSTs is the enzyme's ability to activate GSH, forming and stabilizing the more reactive thiolate anion. In both the cephalopod and mammalian enzyme, an N-terminal Tyr hydroxyl is involved in the process.[14,22]

Compound **1** (Figure 1) was recently characterized as an inhibitor of human H-PGDS[23] and exhibited a therapeutic effect when used in animal models of allergic disease[24,25] and neuroinflammation.[10] The X-ray crystal structure of H-PGDS with **1** and GSH bound was also determined (PDB code 2CVD) and identified the inhibitor binding site as the putative PGH_2 binding site/H site. A cryptic binding site required to accommodate the inhibitors diphenyl moiety was also exposed.[23] More recently, a fragment-based drug design approach identified a number of new H-PGDS inhibitors, including compounds **2** and **3** that bind within the active site cavity without inducing a conformational change.[26] The specificity of these previously reported H-PGDS inhibitors has been assessed in a limited way however. In this study, we developed and characterized a novel series of potent and selective H-PGDS inhibitors that may have applications in allergy-related diseases.

Results

Biochemical Characterization of Inhibitors. A range of distinct H-PGDS inhibitors have recently been reported (compound **1**,[23] compounds **2** and **3**,[26] and compound **4**,[27] Figure 1a), and their binding modes were determined by X-ray crystallography. All compounds were revealed to bind in the prostaglandin binging site, and notably, a cryptic pocket was identified in the X-ray crystal structure of **1** that accommodates a ligand phenyl group and is created by displacement of the Trp104 side chain. By contrast, the compounds developed by fragment based drug design (compounds **2** and **3**) were more planar, did not induce the cryptic pocket, and identified a hydrogen bond donor site in an ordered water molecule, a site not used by **1** (Figure 1b). We characterized compounds **1**, **2**, **3**, and **4** with respect to the H-PGDS CDNB conjugating activity; the data are presented in Table 1. These data indicate that the previously identified H-PGDS inhibitors, compounds **1**, **2**, and **3**, are low to submicromolar inhibitors of the CDNB conjugation reaction. Compound **2** is more potent than either **1** or **3**, while the smaller compound **4** is a weaker inhibitor still. Notably, compounds **2** and **3** exhibit the same rank order against CDNB as against another surrogate substrate, monochlorobimane,[26] while the IC_{50} for **1** (3.8 μM) is similar to that reported for inhibition of PGD_2 synthesis by the purified enzyme (IC_{50} of 6 μM).[23]

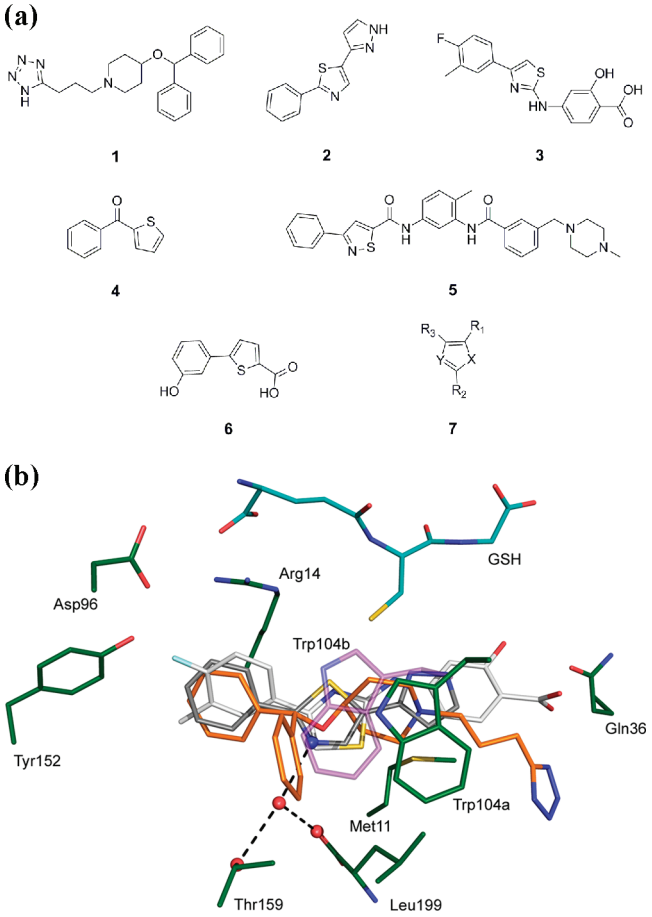

Figure 1. (a) Structures of H-PGDS inhibitors. (b) Structure based alignment. Compound **1** is rendered as orange sticks, compound **2** as gray sticks, and compound **3** as white sticks. Key active site residues are colored green and taken from the crystal structure with compound **1** bound (2CVD). The alternative positions of Trp104 are shown. Trp104a (green) represents the side chain position with compound **1** bound, while Trp104b (purple) illustrates the side chain position in the structures with compounds **2** and **3** bound. Atoms interacting with an ordered water are displayed as spheres, and the interactions are indicated by dashed lines. Of compounds **1**, **2**, and **3**, only compound **2** interacts with the water molecule. The figure was created with PyMol (www.pymol.org).

To explore the possibility of blending these two inhibitor classes, a structure based alignment of **1**, **2**, and **3** (PDB codes 2CVD for **1**, 2VCX for **2**, and 2VD1, for **3**) was generated by a Cα based superposition of the monomers (Figure 1b). The H-PGDS active site was previously described as transitioning from a clearly defined inner cavity to a broad, peripheral solvent exposed component.[26] The molecular alignment demonstrated that the phenyl group of **1** occupying the inner cavity superimposed well with the buried aromatic centers of **2** and **3**, while the two other rings of **2** and **3** traversed the broader solvent exposed region also occupied by the piperazine and alkyl linker of **1**. This indicated the potential for replacement of the piperazine and alkyl chain of **1** with a biphenyl moiety, a concept also supported by **5**, which contains an arrangement of aromatic centers likely to extend beyond the active site space occupied by the substructure common to **2** and **3**, thus capturing the unique interaction between the diphenyl moiety of **1** and the cryptic binding pocket in the PGH_2 binding site, on a biphenyl scaffold.

Table 1. Variation of the Diphenyl Containing Series[a]

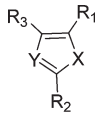

7

Compound	R_1	R_2	R_3	X	Y	$I_{[50]}$	IC_{50} (μM)
1						73.9 ± 2.4	3.8 ± 1.1
2						97.7 ± 0.8	0.7 ± 1.3
3						94.6 ± 3.5	1.4 ± 1.1
4						83.5 ± 1.8	12.8 ± 1.2
6						25.9 ± 3.0	-
8	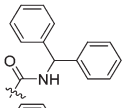		H	S	C	79.2 ± 1.8	0.7 ± 1.0
9	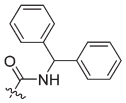		H	S	C	76.4 ± 1.3	1.9 ± 1.1
10	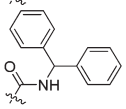		H	S	C	19.9 ± 2.6	-
11	H		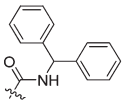	S	N	71.2 ± 4.2	10.8 ± 1.6
12	H		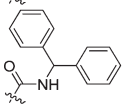	S	N	10.8 ± 1.4	-
13	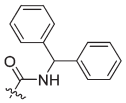		H	C=C	C	6.27 ± 1.9	
14	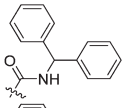	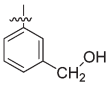	H	S	C	43.8 ± 3.6	-
15	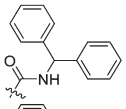		H	S	C	1.8 ± 2.2	-
16	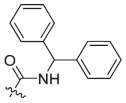		H	S	C	57.9 ± 3.1	-

[a] Inhibition data were determined using the CDNB conjugating activity of purified recombinant human H-PGDS enzyme. IC_{50} values were calculated from triplicate experiments and are presented as IC_{50} ± standard error of the mean. I_{50} is percent inhibition at 50 μM and is presented as the mean ± standard error of triplicate experiments. "−" indicates that IC_{50} values could not be retrieved under the assay conditions.

A low molecular weight fragment that weakly inhibited the CDNB conjugating activity of H-PGDS (approximately 26% at 50 μM), suitable for attachment of a diphenyl group, was identified in **6**, and docking calculations using the protein structure 2CVD predicted that the composite compound, **8**, was likely to adopt a binding mode similar to that of **1**. Few of the interactions identified for compounds **2** and **3**,[26] however, were likely to be made (Figure 2). Clashes were observed in the predicted binding mode between the benzyl ring in the cryptic pocket and Thr159, between the amide carbonyl and Leu199, and between the phenol ring and Met11, while a hydrogen bond was predicted between the side chain carbonyl of Gln36 and the phenol OH of **8**. An interaction with this residue was also observed with the benzylic acid and alcohol moieties of **3**, although these were to the side chain amino group of Gln36. It was unclear if these predicted clashes represent a barrier to ligand binding.

A range of compounds exploring substitutions on the biphenyl moiety were synthesized around a core fragment represented by **7**, and their ability to inhibit purified H-PGDS was tested against the enzyme's GSH conjugating activity; the results are presented in Table 1. An IC_{50} of 0.7 μM was retrieved for the most potent compound, **8**, with the next strongest being **9** (IC_{50} = 1.9 μM). These results demonstrate the importance of a hydrogen bond interaction between the ligand and target site, an interaction was also supported by a striking reduction in I_{50} values in the absence of a donor moiety (compound **10**). Interestingly, a thiazole substitution of the

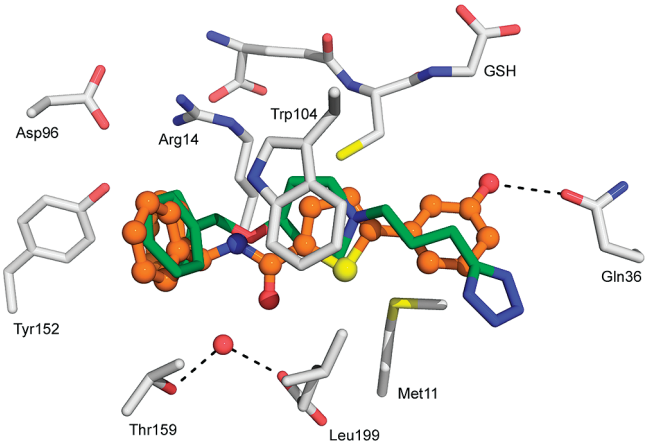

Figure 2. Superimposition of the top ranking binding mode predicted by GOLD for compound **8** (orange ball and stick) onto the crystal structure of compound **1** (green stick) bound to the H-PGDS active site. Figure created with PyMol (www.pymol.org).

central thiophene ring caused an 11-fold reduction in IC_{50} (**11**, 10.8 μM), and potency was further decreased in the absence of a hydrogen bond donor group (**12**), as seen by the decrease in I_{50} values, further supporting the essential nature of this hydrogen bond interaction. Replacement of the central five-membered ring with a benzyl group did not improve the I_{50} (**13**). The position and orientation of the hydrogen bond interaction appear to be restricted, as inclusion of a methylene spacer (**14**) caused a substantial decrease in I_{50} and an acceptor function (**15**) reduced it further. Restricting the orientation of the donor group (**16**) also reduced I_{50}.

The phenol-thiophene scaffold of **8** was further investigated by the addition of a range of amino acids that included Gly, Leu, Phe, Tyr, and Trp, and the results for compounds **17**−**21** (Table 2) demonstrate that an amino acid is tolerated and that an aromatic moiety is preferred, with increases in potency up to approximately 6-fold with respect to the Gly substitution (**17**). Notably, compounds **20** and **21** indicate a positive effect of a hydrogen bond donor group at this position. The phenyl thiophene core was further modified by the addition of a cyclohexyl group, compound **22**, and exhibited only weak H-PGDS inhibition.

The central thiophene ring of **19** was replaced by a phenyl (**23**) and retrieved a comparable IC_{50} (3.7 μM vs 4.6 μM, respectively; Table 2), and this substitution did not alter the preference for an aromatic amino acid component (compounds **24**, **25**, **26**, **27**, and **28**). Replacement of the phenol with an indole hydrogen bond donor group (compound **29**) caused a severe reduction in inhibition. Furthermore, the introduction of an additional donor group on the central phenyl group (compounds **30** and **31**) did not improve the potency of compound **23**, although **31** did clearly demonstrate that substitutions on the 2 position of the central ring are detrimental to activity, giving an I_{50} of only 20%. Reorientation of the biphenyl core also caused a severe reduction in activity (compound **32**), illustrating that the para substituted biphenyl moiety is important for ligand binding. As a biphenyl moiety is well tolerated in the presence of an amino acid, two alternative ring combinations were tested (**33**, **34**), with **34** retrieving an IC_{50} of 1.2 μM (comparable with **24** and **20**), indicating that a phenol hydroxyl group is not essential for strong activity.

Cell-Based Screening Assays. We next assessed the ability of a selection of potent compounds to inhibit inducible PGD_2 production in two inflammation-relevant cell models, mouse primary bone marrow-derived macrophages (BMM) responding to the Toll-like receptor (TLR) 4 agonist lipopolysaccharide (LPS) and the human megakaryocyte cell line MEG-01S responding to PMA differentiation, followed by stimulation with the calcium ionophore A23187. As PGD_2 is produced by both H-PGDS and the genetically distinct L-PGDS, quantitative RT-PCR was first used to assess relative mRNA levels as an indicator of enzyme expression in these cell lines. Figure 3 shows that H-PGDS mRNA was expressed at much higher levels than L-PGDS (1000×) in both mouse BMM and human MEG-01S cells (Figure 3A, Figure 3B). Others have reported that LPS, a TLR4 agonist, induces L-PGDS expression in macrophages,[28,29] and we confirmed that finding here (Figure 3D) and showed that H-PGDS was also regulated by LPS (Figure 3C). Nonetheless, the increase in L-PGDS mRNA expression in response to LPS was very modest in comparison to the high basal expression of H-PGDS in BMM. We conclude that H-PGDS is likely the major PGDS expressed by both human MEG-01S cells and mouse BMM, implying that this enzyme is likely to be the dominant source of PGD_2 production in these cell types.

A selection of compounds was screened for their ability to inhibit PGD_2 production in LPS/TLR4-activated BMM (Figure 4A). Only compounds **19** and **34** significantly inhibited LPS-inducible PGD_2 production in these cells. Both of these compounds had phenylalanine substituted aromatic cores but differed in that **19** had a thiophene-phenol core while **34** possessed a pyridyl-thiophene unit. Strikingly compound **8**, which contained a diphenyl group similar to **1**, showed no inhibitory activity in cells under the conditions tested. Neither **19** nor **34** affected BMM viability at 10 μM, as assessed by MTT assay (Figure 4B), although at 100 μM, **19** greatly reduced cell viability, while compound **34** again showed no cytotoxicity (Figure 4B). Compounds **1** and **2**, identified by others as H-PGDS inhibitors,[24−26] had modest but significant effects at reducing BMM cell viability at 100 μM (Figure 4B).

Compound **34** was further characterized along with the H-PGDS inhibitors **1**[23] and **2**[26] in LPS-activated BMM; the results are presented in Figure 5. Compound **34** inhibited PGD_2 production dose-dependently in the submicromolar range (Figure 5A). The EC_{50} estimated for compound **34** (~0.29 μM) was comparable to that estimated for compound **2** ($EC_{50} \approx 0.16$ μM) and was ~30-fold better than that estimated for **1**. The specificities of **34**, **2**, and **1** were then assessed by comparing effects on LPS-inducible PGE_2, the hydrated prostacyclin derivative 6-keto $PGF_{1\alpha}$, and the thromboxane A_2 derivative TXB_2 production from BMM (Figure 5B,C,D). Compound **1** showed no differential effect in inhibition of PGD_2 versus PGE_2, 6-keto $PGF_{1\alpha}$, or TXB_2, while compound **2** showed only a modest difference. In contrast, compound **34** demonstrated a striking selectivity, inhibiting PGD_2 levels at less than 1 μM, while PGE_2, 6-keto $PGF_{1\alpha}$, and TXB_2 inhibition was only observed above 10 μM. Taken together, these data demonstrate that compound **34** displays selectivity and affinity not otherwise observed for other H-PGDS inhibitors. Furthermore, compounds **2** and **34** also inhibited A23187-inducible PGD_2 production from PMA-differentiated MEG-01S human megakaryocytes dose-dependently, while **1** displayed modest activity at 100 μM (Figure 6A). None of the compounds tested (compound **1**, **2**, or **34**) affected MEG-01S cell viability (Figure 6B), suggesting that inhibition of PGD_2 production occurred through enzyme inhibition.

PGD_2 is the product of a biosynthetic pathway, the first step of which is the release of arachidonic acid from the plasma

Table 2. Variation of the Phenyl Thiophene Series[a]

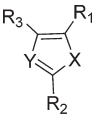

7

Compound	R_1	R_2	R_3	X	Y	$I_{[50]\,\mu M}$	IC_{50} (μM)
17	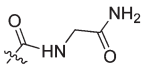		H	S	C	73.9 ± 2.4	8.0 ± 1.2
18	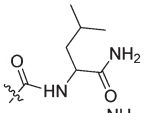		H	S	C	66.9 ± 2.3	7.1 ± 1.2
19	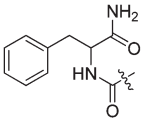		H	S	C	89.5 ± 1.6	3.7 ± 1.0
20	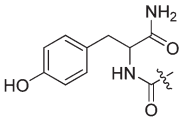		H	S	C	91.3 ± 2.9	1.3 ± 1.0
21	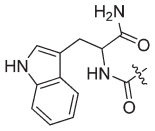		H	S	C	72.5 ± 2.4	2.1 ± 1.2
22	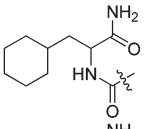		H	S	C	5.07 ± 1.4	-
23	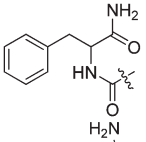		H	C=C	C	88.5 ± 0.6	4.6 ± 1.0
24	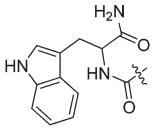		H	C=C	C	91.0 ± 0.4	1.0 ± 1.1
25	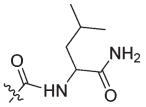		H	C=C	C	57.6 ± 5.1	-
26	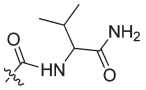		H	C=C	C	53.3 ± 0.6	-
27	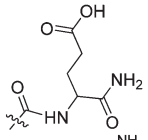		H	C=C	C	-	23.0 ± 1.3
28	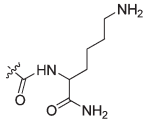		H	C=C	C	24.6 ± 3.0	-
29	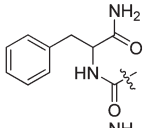		H	C=C	C	14.7 ± 3.6	-
30	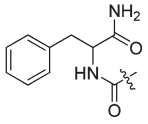		H		C	61.3 ± 0.6	24.8 ± 1.7

Table 2. Continued

Compound	R_1	R_2	R_3	X	Y	$I_{[50]\,\mu M}$	IC_{50} (μM)
31	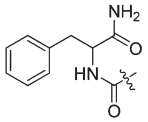		H		C	20.5 ± 5.6	-
32	H		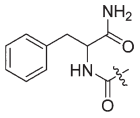	C=C	C	38.0 ± 4.9	-
33	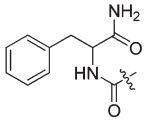		H	C=C	C	54.0 ± 1.4	-
34	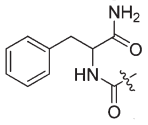		H		C	97.0 ± 2.4	1.2 ± 1.0

[a] Inhibition data were determined using the CDNB conjugating activity of purified recombinant human H-PGDS enzyme. IC_{50} values were calculated from triplicate experiments and are presented as IC_{50} ± standard error of the mean. I_{50} is percent inhibition at 50 μM and is presented as the mean ± standard error of triplicate experiments. "−" indicates that IC_{50} values could not be retrieved under the assay conditions.

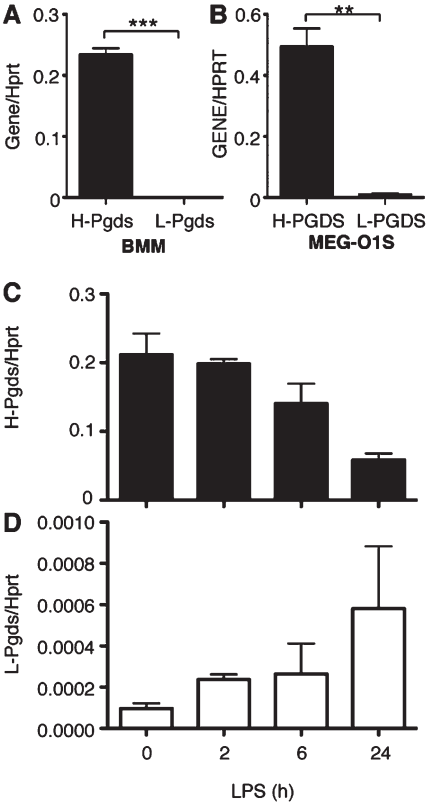

Figure 3. H-PGDS is the predominant PGDS expressed by mouse BMM and human MEG-01S cells. Quantitative RT-PCR data from BMM (A) and MEG-01S cells (B) show the relative mRNA expression levels of H-PGDS versus L-PGDS in unstimulated cells. Data represent the average of three independent experiments plus SEM. BMM were treated with LPS over a 24 h time course, and relative mRNA expression for H-PGDS (C) and L-PGDS (D) was quantitated. Data show the average plus SEM for three independent experiments: (∗∗) $p < 0.01$, (∗∗∗) $p < 0.001$ (Student's *t* test).

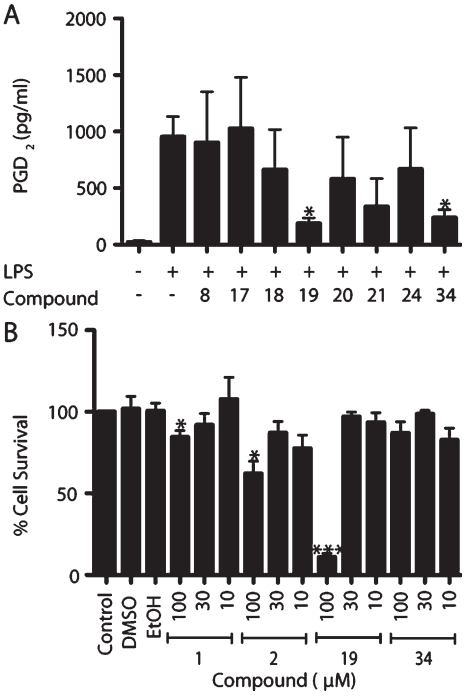

Figure 4. Identification of H-PGDS inhibitors with activity in BMM. BMM were treated with 10 μM compound and LPS (10 ng/mL) for 24 h (A). The average PGD_2 production from three independent experiments plus SEM is shown: (∗) $p < 0.05$ versus LPS treatment alone (Student's *t* test). Compounds that showed significant inhibition of PGD_2 synthesis were used to treat BMM at three doses (10, 30, 100 μM) in the presence of LPS for 24 h, and cell viability was measured by MTT assay (B). Data show the average of four independent experiments plus SEM: (∗) $p < 0.05$, (∗∗∗) $p < 0.001$ versus LPS treatment alone (one sample *t* test where the hypothetical mean is 100).

membrane by phospholipases,[30] followed by conversion to the H-PGDS/L-PGDS substrate PGH_2 by the cyclooxygenase enzymes COX1 and COX2. Inhibition of COX1 and/or COX2 may also have a negative impact on PGD_2 production in cells; therefore, we screened our compounds against purified COX1 and COX2 (Figure 7). Both **34** and a representative from the diphenyl series (**8**) were tested along with **2** and the well-characterized COX inhibitor indomethacin. No inhibition of either COX isoform was observed for the H-PGDS inhibitors,

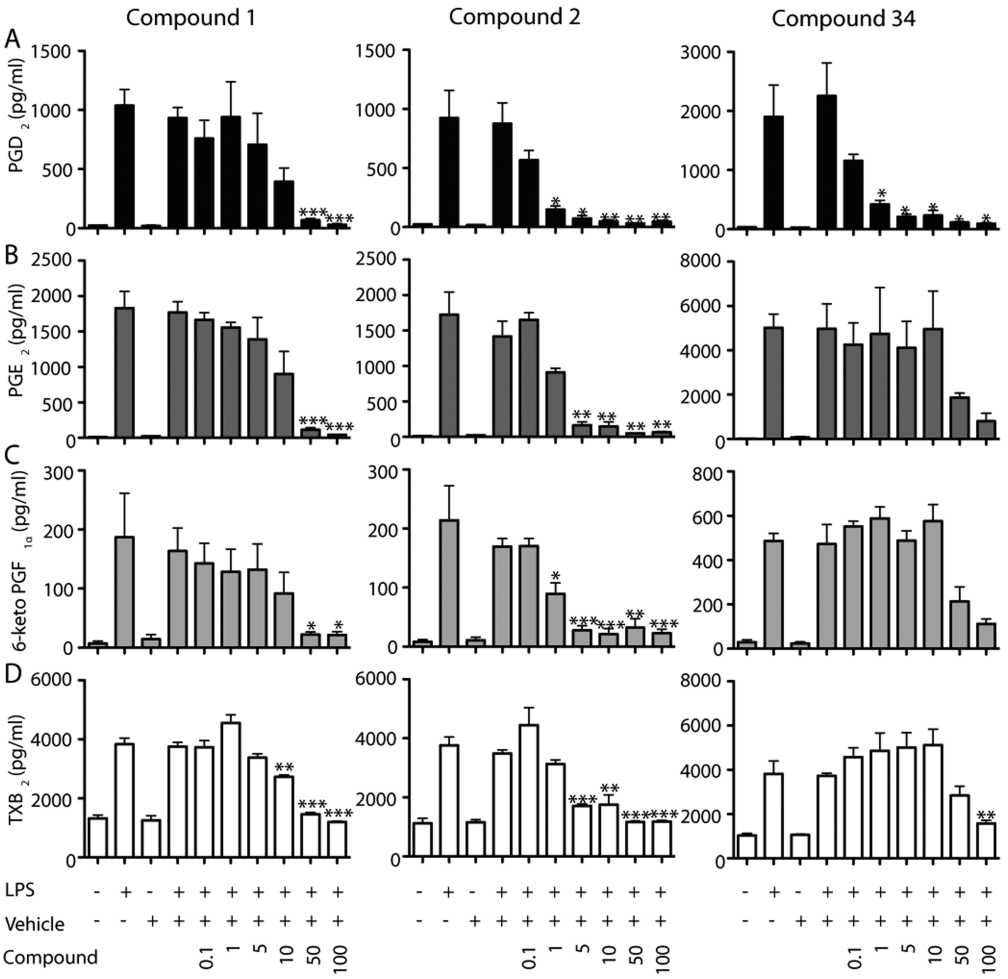

Figure 5. Characterization of prostaglandin inhibition in BMM. BMM were treated with increasing concentrations (0−100 μM) of compounds **1**, **2**, and **34** with appropriate vehicle controls (ethanol for **1**, DMSO for **35** and **2**) and with LPS for 24 h. PGD_2 (A), PGE_2 (B), prostacyclin derivative 6-keto $PGF_{1\alpha}$ (C), and thromboxane A_2 derivative TXB_2 (D) levels in cell culture supernatants were quantified by EIA. Data show the average of three independent experiments plus SEM: (*) $p < 0.05$, (**) $p < 0.01$; (***) $p < 0.001$ (Student's t test) versus vehicle + LPS control.

while indomethacin significantly inhibited the activity of both COX1 and COX2. These data further support the selectivity for inhibition of PGD_2 synthesis of this series of compounds, and altogether, the data indicate that **34** likely blocks PGD_2 synthesis by H-PGDS enzyme inhibition.

Discussion

PGD_2 is the major eicosanoid produced by mast cells after IgE-dependent activation[31] and is readily detected in nasal and bronchial lavage fluids of patients with asthma,[32] allergic rhinitis,[33] atopic dermatitis,[34,35] and allergic conjunctivitis.[36] It triggers a range of biological effects consistent with a pathological role in asthma and allergy, including airways eosinophilia, obstruction, hypersensitivity, and mucus hypersecretion.[8,9,37,38] These inflammatory effects are mediated by interaction with the D prostanoid receptor (DP1) and chemoattractant receptor-homologous molecule expressed on T helper type 2 cell (CRTH2), or DP2. Consistent with a proinflammatory function for PGD_2 in these settings, antagonists of the DP1 and DP2 receptors were therapeutic in animal models of allergic disease.[4,7] The D_2 prostanoid is synthesized by H-PGDS and L-PGDS, two structurally unrelated enzymes,[13,21,39,40] that also differ in tissue expression profiles (refs 12, 13, and 18 and references therein). H-PGDS is highly expressed in mast cells,[41] and as such, it represents an alternative target for modulation of PGD_2 proinflammatory effects.[24,25] Recent studies on H-PGDS in mouse models of neuroinflammation[10] and muscle necrosis[42] also suggest a proinflammatory role for this enzyme in other pathologies. Thus, development of compounds for both receptor and synthase targets will provide unique opportunities to modulate the effects of PGD_2 and is supported by the clinical use of ramatroban, a receptor antagonist,[43] and tranilast, a modest H-PGDS inhibitor,[44] in the control of allergic responses, as well as the therapeutic effect of HQL-79 in animal models of allergic disease.[24,25]

We have been interested in the exploitation of privileged substructures[45−47] and have used a structure guided approach to develop novel H-PGDS inhibitors based on known inhibitory chemotypes, represented by **1**[23] and **2**.[26] Compound **8** was created by the fusion of a diphenyl moiety similar to that of **1** to a weak fragment inhibitor **6**. In doing so, we demonstrated potent inhibition of purified recombinant human H-PGDS, comparable to that of the H-PGDS inhibitor compound **2** and stronger than that of compounds **1** and **3**. While this outcome clearly demonstrates that an effective inhibitor can be developed from the two different moieties and may also favor exposure of a cryptic pocket, it did not exhibit activity in cells. Strikingly, an inhibitor with potency comparable to that of compounds **2** and **3** could also be achieved without the diphenyl moiety and predicted phenol hydroxyl interaction with Gln36, as seen with **34**. In contrast to compound **8**, compound **34**

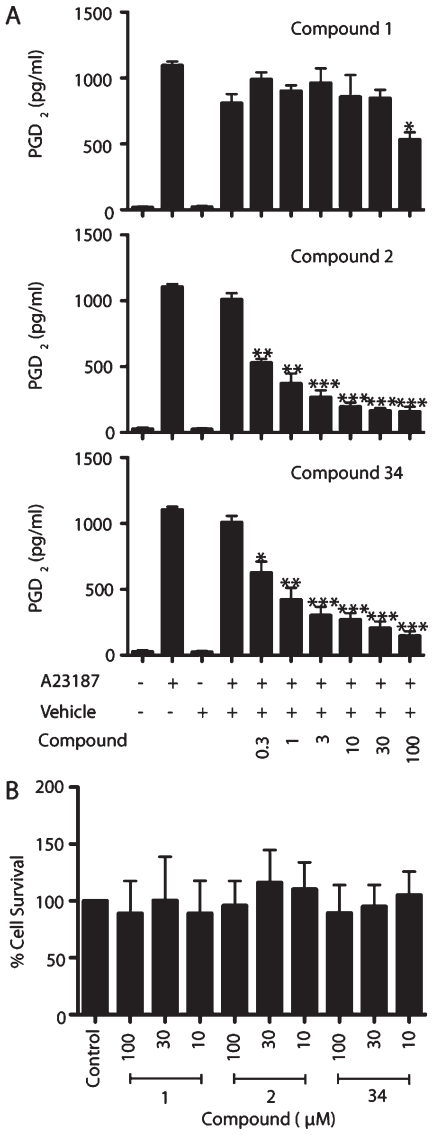

Figure 6. Characterization of prostaglandin inhibition in MEG-01S human megakaryocytes. PMA differentiated MEG-01S were treated with compounds **1**, **2**, and **34** across a range of concentrations (0−100 μM) for 30 min prior to 30 min treatment with 5 μM calcium ionophore A23187. PGD_2 levels in cell culture supernatants were quantitated by EIA (A). Data represent the average of three independent experiments plus SEM: (∗) $p < 0.05$, (∗∗), $p < 0.01$, (∗∗∗) $p < 0.001$ (Student's t test) versus vehicle + ionophore control. The effect of the compounds on MEG-01S cell viability was measured by MTT assay after 24 h of treatment across the concentration range, 0−100 μM, of compounds (B). Data represent the average of four independent experiments plus SEM.

demonstrated inhibition of PGD_2 synthesis in intact cells, with a dose dependent profile similar to that of the recently reported H-PGDS inhibitor compound **2**. Where inhibition of PGD_2 synthesis was observed in cells, the data were in agreement with rank ordering based on enzyme assay data; IC_{50} values retrieved for compounds **1**, **2**, and **34** ranked them in order of potency **2** > **34** > **1**, an order consistent with their EC_{50} in cells. While these compounds appear slightly more active in the cellular assay, for example, compound **34** is 4-fold more potent in cell-based assays than in enzyme assays with a similar dose dependent activity in human and mouse cell types, this is likely due to the different assay systems employed. Comparison of the relative differences in IC_{50} values retrieved for compounds **2** and **3**

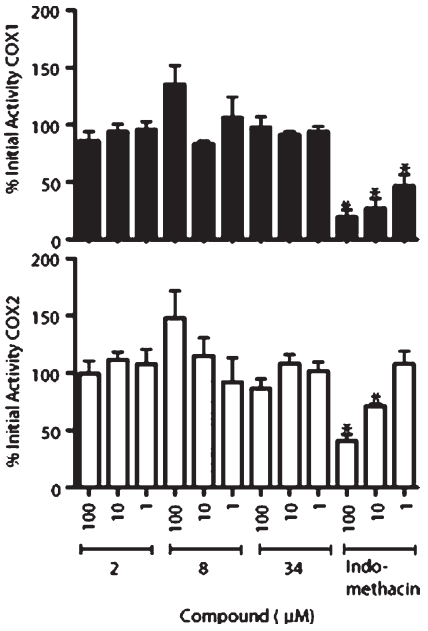

Figure 7. Characterization of COX1 and COX2 inhibiton. Two novel H-PGDS inhibitors, compounds **8** and **34**, were assayed for possible inhibition of purified COX1 and COX2 isoforms at 1, 10, and 100 μM, along with the known inhibitor of COX 1 and COX2, indomethacin. Data represent the average of three independent experiments plus SEM: (∗) $p < 0.05$ (one sample t test where the hypothetical mean is 100).

in this study (2×) to those previously reported (6.5×)[26] also supports this. Notably, the less potent H-PGDS inhibitor, compound **1**, showed differences in efficacy across the cell types used, having a greater effect in mouse macrophage over human megakaryocyte. The human and mouse H-PGDS isoforms exhibit 80% sequence identity, with residues contributing to the active site cavity being mostly conserved. Three positions that vary between the two enzymes include Glu41Lys, Ser44-Pro, and Phe163Leu (human vs mouse). The Glu41Lys and Ser44Pro substitutions occur in the α2 helix, a secondary structure element associated with GSH binding, while the Phe163-Leu residue contributes to the cryptic pocket and is in proximity to the buried phenyl group of compound **1**. This variation may alter the interaction of compound **1** with the cryptic pocket and contribute to the difference in efficacy observed between mouse and human cells.

Prostaglandin E synthase, prostacyclin synthase, thromboxane synthase, and H-PGDS all use the COX product PGH_2 as a precursor for their own prostanoid products, and loss of these downstream prostaglandins is a likely cause of side effects associated with COX inhibitors.[6,48] Thus, analysis of the effects of H-PGDS inhibitors on the production of other prostaglandins, prostacylcins, and thromboxanes is clearly warranted. We addressed this issue by measuring inducible PGD_2 versus PGE_2, PGI_2 (by measuring its derivative 6-keto $PGF_{1\alpha}$), and TXA_2 (by measuring its derivative TXB_2) production in LPS-activated BMM and demonstrated that **34** showed selectivity for inhibiting PGD_2 production, while that for other reported H-PGDS inhibitors was more modest. The selective inhibition of LPS-inducible PGD_2 synthesis was also supported by the absence of COX1 and COX2 inhibition.

The induction of L-PGDS in macrophages by LPS has been previously characterized,[28,29] and we confirmed those findings here by examining L-PGDS mRNA levels across an LPS time-course. While L-PGDS silencing indicated that enzyme as the

main source of PGD_2 upon LPS stimulation of a macrophage derived cell line,[29] our transcriptional profiling and inhibition studies support H-PGDS as the main source of PGD_2 synthesis in isolated mouse bone marrow derived macrophages activated similarly. Notably, residual PGD_2 synthesis was observed in both cell types for compounds **1**, **2**, and **34**, suggesting that under the conditions tested, some PGD_2 synthesis may occur through a H-PGDS independent pathway and is consistent with low expression of L-PGDS. Thus, these compounds represent novel reagents for probing the function of H-PGDS activity in both normal physiological and disease states.

Experimental Section

Materials. Glutathione, 1-chloro-2,4-dinitrobenzene, indomethacin, and nocodazole were purchased from Sigma-Aldrich Pty Ltd. (Castle Hill, NSW, Australia). Compound **1** was obtained from Cayman Chemical (Ann Arbor, MI). Compound **2** was purchased at Ryan Scientific (Mt. Pleasant, SC).

Protein Expression and Purification. Human H-PGDS was expressed and purified as described previously.[18] Briefly, H-PGDS was expressed in *Escherichia coli* strain BL21 DE3 transformed with the pET17b HPGDS expression construct, grown overnight at 37 °C in 250 mL of Luria−Bertani medium supplemented with 100 μg/mL ampicillin. After 24 h, without induction, bacteria were harvested by centrifugation at 5000*g* for 20 min at 4 °C; cell pellets were kept at −70 °C until required. Cells were resuspended in 25 mL of ice-cold phosphate buffered saline (PBS), pH 7.4, containing 1 mM DTT, 0.5% Triton X-100, and EDTA-free protease inhibitor tablets (F. Hoffmann-La Roche, Dee Why, NSW, Australia), and incubated with rotation for 30 min at 4 °C. Cells were then lysed by sonication at 90−100 W over 3 × 1 min intervals while incubating on ice; the lysate was then clarified by centrifugation at 18000*g* for 10 min at 4 °C.

The supernatant was then applied to a GSTPrep FF 16/10 column pre-equilibrated with PBS, pH 7.4, and 1 mM DTT, at 0.4 mL/min using an AKTA explorer 100 (GE Healthcare, Rydalmere, NSW, Australia), then washed with 5 column volumes of the same buffer at 1 mL/min. Bound H-PGDS was eluted in 5 column volumes of 15 mM reduced glutathione in 50 mM Tris, pH 9.0, at 0.5 mL/min and dialyzed against 100 volumes of 5 mM Tris/HCl, pH 8.0. The protein was concentrated to 20 mg/mL, as determined by the method of Bradford[49] using an Amicon Ultra-4 centrifugal filter device (Millipore, North Ryde, NSW, Australia) following the manufacturer's recommendations. Glycerol was added to a final concentration of 10% (v/v) prior to storage at −20 °C.

Enzyme Assays. The H-PGDS catalyzed conjugation of GSH and CDNB was used as the biochemical assay for enzyme inhibition. Reactions were performed in 96-well plate format, and product formation was followed at A340 nm over a 10 min interval at 25 °C using a POWERWAVE XS microplate scanning spectrophotometer (Bio-Tek Instruments, Winooski, VT). Reactions were performed in 0.1 M Tris HCl, pH 8.0, containing 2 mM $MgCl_2$, 1 mM CDNB, 2 mM GSH, 2.5 ng/μL purified H-PGDS, and 10% (v/v) ethanol in a 200 μL reaction volume. IC_{50} values were calculated from rates of conjugation activity determined at eight concentration points bracketing the IC_{50}, where compound solubility allowed, and were corrected for background activity at the same solvent concentrations. All compounds were made up in 100% DMSO and diluted with 0.1 M Tris HCl, pH 8.0, with 2 mM $MgCl_2$. I_{50} and IC_{50} values were determined at a final DMSO composition of no greater than 4% v/v for all compounds. Nonlinear regression analysis and IC_{50} calculations were performed using GraphPad Prism, version 4.0c. COX1 and COX2 enzyme assays were performed using the colorimetric COX (ovine) inhibitor screening assay kit (Cayman Chemical) according to the manufacturer's instructions.

Cell Culture. All bone marrow-derived macrophages (BMM) were obtained by culturing bone marrow cells from the femurs of 6- to 8-week-old C57BL/6 male mice in RPMI 1640 medium (Invitrogen Life Technologies, Carlsbad, CA) supplemented with 10% fetal calf serum (Invitrogen), 20 U/mL penicillin and 20 μg/mL streptomycin (Invitrogen), 2 mM L-glutamine (Glutamax-1, Invitrogen) in the presence of 10^4 U/mL (100 ng/mL) recombinant human CSF-1 (a gift from Chiron, Emeryville, CA) on bacteriological plastic plates for 7 days. The human megakaryocytic cell line MEG-01S was obtained from the American Type Culture Collection. MEG-01S cells were maintained in the same media as for BMM but was additionally supplemented with 1 mM sodium pyruvate (Invitrogen).

Determination of mRNA Expression by Quantitative PCR (qPCR). RNA was extracted from 3×10^6 cells and cDNA synthesized as described previously.[50] Briefly, RNA was extracted using RNeasy kits (Qiagen, Valencia, CA), contaminating genomic DNA removed using RNeasy on-column DNase (Qiagen), and cDNA was synthesized using Superscript III (Invitrogen) and oligo(dT) primer. Transcript abundance was quantitated using gene-specific primer pairs and the SYBR green system (Applied Biosystems, Foster City, CA) relative to hypoxanthine guanine phosphoribosyl transferase (HPRT) levels using the power δ Ct method. Primer efficiencies for the respective human and mouse H-PGDS and L-PGDS primer pairs were measured over a cDNA dilution series and were used to normalize expression such that comparisons could be made of mRNA levels for H-PGDS versus L-PGDS (for human and mouse). Primer pairs used were human *H-PGDS* gene (forward TCACCAGAGCCTAGCAATAGCA, reverse CTGCCCAAGGAAAACATGACA); human *L-PGDS* gene (forward CCTGACCTCCACCTTCCTCA, reverse TCGGTCTCCACCACTGACAC); human *HPRT* gene (forward TCAGGCAGTATAATCCAAAGATGGT, reverse AGTCTGGCTTATATCCAACACTTCC); mouse *H-pgds* gene (forward AAGCACCTCGCCTTCTGAAA, reverse CAGTAGAAGTCTGCCCAGGTTACAT); mouse *L-pgds* gene (forward CAGAGGGCTGGTCACATGGT, reverse AGGCAAAGCTGGAGGGTGTAG); mouse *Hprt* gene (forward GCAGTACAGCCCCAAAATGG, reverse AACAAAGTCTGGCCTGTATCCAA).

Prostaglandin Release from Cells. BMM were seeded overnight at 2×10^5 cells/mL in 24-well plates before treatment with compound at either 10 or 0.1−100 μM for 24 h in the presence or absence of lipopolysaccharide (LPS) from *Salmonella minnesota* (Sigma-Aldrich) at a final concentration of 10 ng/mL. MEG-01S was seeded at 2×10^5 cells/mL and stimulated with PMA (phorbol 12-myristate 13-acetate) (Sigma-Aldrich) at a final concentration of 0.1 μM for 16 h. Compound (0.3−100 μM) was added 30 min prior to stimulation with 5 μM calcium ionophore A23187 (Sigma-Aldrich) for 30 min. All compounds were dissolved in DMSO and diluted in cell culture medium such that the final concentration of DMSO did not exceed 0.1%. Supernatants were collected, and samples were analyzed for PGD_2 using prostaglandin D2 MOX Express EIA kits, for PGE_2 using prostaglandin E2 Express EIA kits, for the prostacyclin derivative 6-keto $PGF_{1\alpha}$ using the 6-keto prostaglandin $F_{1\alpha}$ EIA kit and the thromboxane A_2 derivative TXB_2 using the thromboxane B_2 Express EIA kit (Cayman Chemical) according to the manufacturer's instructions.

Cell Viability Assays. BMM were seeded at 1×10^5 cells/well in 96-well plates and treated for 24 h with LPS (10 ng/mL) and compounds at 10, 30, and 100 μM. MEG-01S was PMA differentiated overnight before compounds were added for a further 24 h at 10, 30, and 100 μM. Cell viability was measured by MTT (Sigma-Aldrich) assay as described previously.[51]

Chemical Methods. General Procedure. Nuclear magnetic resonance spectra were recorded at 400 MHz (^{1}H)/100 MHz (^{13}C) on a Varian Gemini-400. ^{1}H and ^{13}C chemical shifts (δ) are given in parts per million (ppm) using residual protonated solvent (DMSO-d_6) as an internal standard. Coupling constants are given in hertz (Hz). The following abbreviations are used: s = singlet, d = doublet, t = triplet, m = multiplet, bs = broad signal. Low resolution mass

spectral data were recorded on a API2000 (TOF MS ES+) instrument (Applied Biosystems). High resolution mass spectral data were obtained on a PE Sciex API QSTAR Pulsar (ES-qTOF) (Perkin-Elmer, Waltham, MA) instrument using ACP (acyl carrier protein) (65−74) ($C_{47}H_{75}N_{12}O_{16}$ (M + H), 1063.5424) and reserpine ($C_{33}H_{40}N_2O_9$ (M + H), 609.2812) as internal references. Resolution for the instrument was set between 10 000 and 12 000 for all standards. Analytical reversed-phase high performance liquid chromoatography (HPLC) was performed on a Gemini C_{18} column (4.6 mm × 250 mm) (Phenomenex, Lane Cove, NSW, Australia). Preparative reversed phase HPLC was performed on a Gemini 10 μm C_{18} column (22 mm × 250 mm) (Phenomenex) or Jupiter 10 μm, 300 Å C_{18} column (21.2 mm × 250 mm) (Phenomenex). Separations were achieved using linear gradients of buffer B in A (A = 0.1% aqueous TFA; B = 90% CH_3CN, 10% H_2O, 0.09% TFA) at a flow rate of 1 mL/min (analytical) and 20 mL/min (preparative).

Rink amide resin (sv = 0.65 mmol/g), 2-(1*H*-benzotriazol-1-yl)-1,1,3,3-tetramethyluronium hexafluorophosphate (HBTU), and all N_α-Fmoc-amino acids were peptide synthesis grade purchased from IRIS Biotech (Marktredwitz, Germany). Dichloromethane, diisopropylethylamine, *N*,*N*-dimethylformamide, and trifluoroacetic acid were obtained from Auspep (Parkville, VIC, Australia). HPLC grade acetonitrile and methanol were purchased from Labscan (Gliwice, Poland). All other reagents and solvents were purchased from Sigma-Aldrich, Alfa Aesar (Lancashire, England), Combi-Blocks (San Diego, CA), Oakwood Products (West Columbia, SC), Frontier Scientific (Logan, UT), Boron Molecular (Noble Park, VIC, Australia), and Trans World Chemicals (Rockville, MD).

General Procedure A (On-Resin Synthesis). Preparation of Biaryls. For formation of resin-bound bromide, functionalized Rink amide polystyrene resin (0.325 mmol, 0.5 g) was derivatized with Fmoc-AA using in situ neutralization/HBTU activation protocols for Fmoc chemistry.

For formation of biaryl, bromo-functionalized resin (0.325 mmol) was placed in a reaction vessel under nitrogen atmosphere. DME (5 mL) was degassed and added to the resin, followed by addition of neat $Pd(PPh_3)_4$ (81 mg, 0.07 mmol). A solution of the boronic acid (1.3 mmol) in degassed EtOH (1 mL) was added to the resin, and the mixture was agitated for 5 min; CsF (162 mg, 1.3 mmol) was added neat. The mixture was agitated 16 h at 60 °C before excess reagents were removed by filtration, and the resin was washed with DMF (3×) and DCM (3×) to yield resin bound compound.

General Procedure for Amide Bond Coupling. All amide bond couplings were chemically synthesized using Fmoc protecting groups and in situ HBTU activation protocols.

Cleavage off Resin. The resin was dried for several hours under reduced pressure and placed in a cleavage vessel. The resin was treated with a mixture of TFA/H_2O 92:8 for an hour. TFA was blown off under nitrogen atmosphere, and the dry cleaved crude product was redissolved in solvent A/B and separated from the resin. Preparative HPLC of the final product followed by lyophilization gave a white powder (>95% by analytical HPLC). Preparative separations were achieved using a linear gradient (1%/min) of buffer B in A (A = aqueous 0.045% TFA; B = 90% CH_3CN, 10% H_2O, 0.045% aqueous TFA) at a flow rate of 20 mL/min. Analytical HPLC was achieved using a linear gradient (3%/min) of buffer B in A (A = aqueous 0.045% TFA; B = 90% CH_3CN, 10% H_2O, 0.045% aqueous TFA) at a flow rate of 1 mL/min. Compounds obtained were determined to be >95% pure by analytical HPLC.

General Procedure B (Solution Based Synthesis). Preparation of Biaryls. A mixture of organoboronic acid (2.35 mM) and an ester bromide (2.39 mmol) was dissolved in toluene (15 mL), and then CsF (1.51 g, 10.0 mmol) was added. The catalyst $Pd(PPh_3)_4$ (35 mg, 0.03 mmol) and CuI (4%, 15 mg, 0.02 mmol) were added, and the flask was evacuated and refilled with argon five times. The mixture was stirred at 80 °C overnight and then diluted with dichloromethane (40 mL) and water (20 mL). After the mixture was vigorously shaken, the mixture was filtered through Celite with DCM/EtOAc (100 mL, 1:1). The organic layer was separated, dried over $MgSO_4$, and the solvent was removed under reduced pressure. Preparative HPLC, followed by freeze-drying, gave the pure product as a white solid material.

General Procedure Hydrolysis. Hydrolysis of the pure fractions was performed with 1 M lithium hydroxide (LiOH) in tetrahydrofuran (THF) for 16 h. The solvent was removed under reduced pressure, providing the compound with a free acid.

General Procedure Amine Coupling. The functionalized carboxylic acid (1 equiv) and benzhydrylamine (2 equiv) were placed in a reaction vessel under nitrogen atmosphere. PyBrOP (2 equiv) was added neat together with DIEA (2.2 equiv) and DMF. The mixture was stirred for 24 h at room temperature. Solvent was removed by evaporation using a GeneVac Atlas HT-8 speed evaporation system. Preparative HPLC of the final product followed by lyophilization gave a white powder (>95% by analytical HPLC). Preparative separations were achieved using a linear gradient (1%/min) of buffer B in A (A = aqueous 0.045% TFA; B = 90% CH_3CN, 10% H_2O, 0.045% aqueous TFA) at a flow rate of 20 mL/min. Analytical HPLC was achieved using a linear gradient (3%/min) of buffer B in A (A = aqueous 0.045% TFA; B = 90% CH_3CN, 10% H_2O, 0.045% aqueous TFA) at a flow rate of 1 mL/min.

***N*-Benzhydryl-5-(3-hydroxyphenyl)thiophene-2-carboxamide (8)** was prepared according to method B except using 3-hydroxyphenylbronic acid (2.35 mmol) and methyl 5-bromothiophene-2-carboxylate (2.39 mmol). Preparative HPLC of the final product followed by lyophilization gave a white powder (>95% purity by analytical HPLC). Yield: 3.7 mg, 23.5%. ^{1}H NMR (400 MHz, DMSO-d_6): δ 6.34 (d, J = 8.8 Hz, 1H), 6.74 (dd, J = 2 Hz, J = 9.6 Hz, 1H), 7.03 (d, J = 3.6 Hz, 1H), 7.11 (dd, J = 2 Hz, J = 8.4 Hz, 1H), 7.21 (t, J = 7.8 Hz, 1H), 7.23 −7.36 (m, 10H), 7.44 (d, J = 4 Hz, 1H), 7.97 (d, J = 4 Hz, 1H), 9.26 (d, J = 8.8 Hz, 1H), 9.64 (bs, 1H). ^{13}C NMR (100 MHz, DMSO-d_6): δ 160.9, 158.4, 148.4, 142.5 (2C), 138.7, 134.7, 130.8, 130.3, 128.8 (4C), 128.1 (4C), 127.5 (2C), 124.5, 117.0, 116.1, 112.8, 56.7. ESI-HRMS calculated for $C_{24}H_{19}NO_2S$ $[M + H]^+$: 386.1215. Found: 386.1229.

5-(3-Aminophenyl)-*N*-benzhydrylthiophene-2-carboxamide (9) was prepared according to method B except using 3-aminophenylbronic acid (2.35 mmol) and methyl 5-bromothiophene-2-carboxylate (2.39 mmol). Preparative HPLC of the final product followed by lyophilization gave a white powder (>95% purity by analytical HPLC). Yield: 25.3 mg, 5.0%. ^{1}H NMR (400 MHz, DMSO-d_6): δ 6.35 (d, J = 8.4 Hz, 1H), 6.88 (dd, J = 3.2 Hz, J = 7.2 Hz, 1H), 7.18 (d, J = 1.6 Hz, 1H), 7.24−7.28 (m, 4H), 7.30−7.37 (m, 10H), 7.46 (d, J = 4 Hz, 1H), 7.99 (d, J = 4.4 Hz, 1H), 9.29 (d, J = 8.8 Hz, 1H). ^{13}C NMR (100 MHz, DMSO-d_6): δ 160.8, 148.9, 148.1, 142.4 (2C), 138.9, 138.2, 134.4, 130.6, 130.2, 128.8 (4C), 128.1 (4C), 127.6 (2C), 118.4, 115.1, 114.1, 57.8. ESI-HRMS calculated for $C_{24}H_{20}N_2OS$ $[M + H]^+$: 385.1338. Found: 385.1345.

***N*-(2-Amino-2-oxoethyl)-5-(3-hydroxyphenyl)thiophene-2-carboxamide (17)** was prepared according to method A except using Fmoc-protected glycine (1.3 mmol), 5-bromo-2-thiophenecarboxylic acid (0.975 mmol), and 3-hydroxyphenylboronic acid (1.3 mmol). Preparative HPLC of the final product followed by lyophilization gave a white powder (>95% purity by analytical HPLC). Yield: 14 mg, 15.6%. ^{1}H NMR (400 MHz, DMSO-d_6): δ 3.77 (d, J = 6 Hz, 2H), 6.75 (dd, J = 2.4 Hz, J = 8.2 Hz, 1H), 7.03 (d, J = 4 Hz, 1H), 7.11 (dd, J = 1.6 Hz, J = 7.8 Hz, 1H), 7.22 (t, J = 15.6 Hz, 1H), 7.37 (bs, 1H), 7.43 (d, J = 3.6 Hz, 1H), 7.74 (d, J = 4 Hz, 1H), 8.7 (t, J = 12 Hz, 1H), 9.64 (bs, 1H). ^{13}C NMR (100 MHz, DMSO-d_6): δ 171.3, 161.7, 158.4, 148.1, 138.7, 134.7, 130.8, 129.9, 124.5, 116.9, 116.1, 112.7, 42.6. ESI-HRMS calculated for $C_{13}H_{12}N_2O_3S$ $[M + H]^+$: 277.0647. Found: 277.0634.

***N*-(1-Amino-4-methyl-1-oxopentan-2-yl)-5-(3-hydroxyphenyl)-thiophene-2-carboxamide (18)** was prepared according to method A except using Fmoc-protected leucine (1.3 mmol), 5-bromo-2-thiophenecarboxylic acid (0.975 mmol), and 3-hydroxyphenylboronic acid (1.3 mmol). Preparative HPLC of the final product

followed by lyophilization gave a white powder (>95% purity by analytical HPLC). Yield: 23 mg, 21.3%. ^{1}H NMR (400 MHz, DMSO-d_6): δ 0.87 (dd, J = 15.6 Hz, J = 6.4 Hz, 6H), 1.51 (m, 1H), 1.61 (m, 2H), 4.39 (m, 1H), 6.72 (dd, J = 4.8 Hz, J = 8.6 Hz, 1H), 6.97 (bs, 1H), 7.03 (d, J = 2.5 Hz, 1H), 7.11 (dd, J = 2.5 Hz, J = 8 Hz, 1H), 7.21 (t, J = 9.3 Hz, 1H), 7.42 (bs, 1H), 7.43 (d, J = 4 Hz, 1H), 7.86 (d, J = 4 Hz, 1H), 8.42 (d, J = 8.4 Hz, 1H), 9.62 (bs, 1H). ^{13}C NMR (100 MHz, DMSO-d_6): δ 174.6, 161.3, 158.4, 148.1, 138.8, 134.8, 130.8, 130.1, 124.5, 116.9, 116.0, 112.7, 51.9, 41.0, 24.9, 23.5, 21.8. ESI-HRMS calculated for $C_{17}H_{20}N_2O_3S$ [M + H]$^+$: 333.1273. Found: 333.1253.

***N*-(1-Amino-1-oxo-3-phenylpropan-2-yl)-5-(3-hydroxyphenyl)-thiophene-2-carboxamide (19)** was prepared according to method A except using Fmoc-protected phenylalanine (1.3 mmol), 5-bromo-2-thiophenecarboxylic acid (0.975 mmol), and 3-hydroxyphenylboronic acid (1.3 mmol). Preparative HPLC of the final product followed by lyophilization gave a white powder (>95% purity by analytical HPLC). Yield: 18.33 mg, 15.41%. ^{1}H NMR (400 MHz, DMSO-d_6): δ 2.93 (dd, J = 13.8 Hz, J = 30 Hz, 1H), 3.06 (dd, J = 13.8 Hz, J = 30 Hz, 1H), 4.57 (ddd, J = 8.4 Hz, J = 13.8 Hz, J = 13.8 Hz, 1H), 6.72 (dd, J = 4.8 Hz, J = 8 Hz, 1H), 7.01 (d, J = 2 Hz, 1H), 7.07−7.27 (m, 7H), 7.3 (bs, 1H), 7.32 (d, J = 1.6 Hz, 1H), 7.4 (d, J = 4 Hz, 1H), 7.55 (bs, 1H), 7.8 (d, J = 4 Hz, 1H), 8.56 (d, J = 8.4 Hz, 1H), 9.62 (bs, 1H). ^{13}C NMR (100 MHz, DMSO-d_6): δ 173.6, 161.2, 158.3, 148.1, 138.9, 138.7, 134.7, 130.7, 130.0, 129.6 (2C), 128.5 (2C), 126.7, 124.5, 116.9, 116.0, 112.7, 55.1, 37.7. ESI-HRMS calculated for $C_{20}H_{18}N_2O_3S$ [M + H]$^+$: 367.1116. Found: 367.1128.

***N*-(1-Amino-3-(4-hydroxyphenyl)-1-oxopropan-2-yl)-5-(3-hydroxyphenyl)thiophene-2-carboxamide (20)** was prepared according to method A except using Fmoc-protected tyrosine (1.3 mmol), 5-bromo-2-thiophenecarboxylic acid (0.975 mmol), and 3-hydroxyphenylboronic acid (1.3 mmol). Preparative HPLC of the final product followed by lyophilization gave a white powder (>95% purity by analytical HPLC). Yield: 29.97 mg, 24.15%. ^{1}H NMR (400 MHz, DMSO-d_6): δ 2.81 (dd, J = 13.7 Hz, J = 30 Hz, 1H), 2.97 (dd, J = 14 Hz, J = 30 Hz, 1H), 4.48 (ddd, J = 8.4 Hz, J = 13.7 Hz, J = 14 Hz, 1H), 6.60 (d, J = 8 Hz, 2H), 6.73 (dd, J = 2.4 Hz, J = 8 Hz, 1H), 7.01 (d, J = 4 Hz, 1H), 7.05 (bs, 1H), 7.07−7.10 (m, 3H), 7.2 (t, J = 15.6 Hz, 1H), 7.41 (d, J = 4 Hz, 1H), 7.5 (bs, 1H), 7.8 (d, J = 4 Hz, 1H), 8.49 (d, J = 8.4 Hz, 1H), 9.12 (bs, 1H), 9.63 (bs, 1H). ^{13}C NMR (100 MHz, DMSO-d_6): δ 173.7, 161.2, 158.3, 156.1, 148.1, 139.1, 134.7, 130.7, 130.5 (2C), 130.1, 128.9, 124.5, 116.9, 116.0, 115.3 (2C), 112.7, 55.4, 37.2. ESI-HRMS calculated for $C_{20}H_{18}N_2O_4S$ [M + H]$^+$: 383.1065. Found: 383.1080.

***N*-(1-Amino-3-(1*H*-indol-3-yl)-1-oxopropan-2-yl)-5-(3-hydroxyphenyl)thiophene-2-carboxamide (21)** was prepared according to method A except using Fmoc-protected tryptophan (1.3 mmol), 5-bromo-2-thiophenecarboxylic acid (0.975 mmol), and 3-hydroxyphenylboronic acid (1.3 mmol). Preparative HPLC of the final product followed by lyophilization gave a white powder (>95% purity by analytical HPLC). Yield: 10.6 mg, 8.1%. ^{1}H NMR (400 MHz, DMSO-d_6): δ 3.06 (dd, J = 10 Hz, J = 14.5 Hz, 1H), 3.18 (dd, J = 4 Hz, J = 14.5 Hz, 1H), 4.62 (ddd, J = 4 Hz, J = 10 Hz, J = 12.8 Hz, 1H), 6.72 (dd, J = 2.2 Hz, J = 8.4 Hz, 1H), 6.95 (t, J = 15.2 Hz, 1H), 7.02 −7.09 (m, 4H), 7.16 (d, J = 2.4 Hz, 1H), 7.19 (t, J = 15.6 Hz, 1H), 7.28 (dd, J = 2 Hz, J = 8.2 Hz, 1H), 7.4 (d, J = 4 Hz, 1H), 7.56 (bs, 1H), 7.67 (d, J = 8 Hz, 1H), 7.8 (d, J = 3.6 Hz, 1H), 8.49 (d, J = 8.4 Hz, 1H), 9.62 (bs, 1H), 10.74 (d, J = 2 Hz, 1H). ^{13}C NMR (100 MHz, DMSO-d_6): δ 174.0, 161.2, 158.3, 148.0, 138.5, 138.1, 136.5, 134.9, 131.1, 130.0, 127.9, 124.4, 123.9, 121.8, 119.0, 117.3, 116.1, 113.1, 112.0, 111.3, 55.3, 28.1. ESI-HRMS calculated for $C_{22}H_{19}N_3O_3S$ [M + H]$^+$: 406.1225. Found: 406.1239.

***N*-(1-Amino-3-(1*H*-indol-3-yl)-1-oxopropan-2-yl)-3′-hydroxybiphenyl-4-carboxamide (24)** was prepared according to method A except using Fmoc-protected tryptophan (1.3 mmol), 4-bromobenzoic acid (0.975 mmol), and 3-hydroxyphenylboronic acid (1.3 mmol). Preparative HPLC of the final product followed by lyophilization gave a white powder (>95% purity by analytical HPLC). Yield: 4.0 mg, 3.1%. ^{1}H NMR (400 MHz, DMSO-d_6): δ 3.12 (dd, J = 4.4 Hz, J = 14.6 Hz, 1H), 3.22 (dd, J = 10 Hz, J = 14.8 Hz, 1H), 4.68 (ddd, J = 4.4 Hz, J = 7 Hz, J = 10 Hz, 1H), 6.78 (dd, J = 2.4 Hz, J = 8 Hz, 1H), 6.96 (t, J = 13.6 Hz, 1H), 7.01−7.10 (m, 4H), 7.18 (d, J = 2.4 Hz, 1H), 7.25 (d, J = 7.6 Hz, 1H), 7.28 (dd, J = 0.8 Hz, J = 7.4 Hz, 1H), 7.54 (bs, 1H), 7.63 (d, J = 5.1 Hz, 2H), 7.66 (d, J = 5.7 Hz, 1H), 7.86 (dd, J = 1.6 Hz, J = 5.7 Hz, 2H), 8.40 (d, J = 8 Hz, 1H), 9.54 (bs, 1H), 10.73 (s, 1H). ^{13}C NMR (100 MHz, DMSO-d_6): δ 174.2, 166.2, 158.3, 143.3, 141.0, 136.5, 133.4, 130.5, 128.5 (2C), 127.8, 126.7 (2C), 124.0, 121.3, 119.0, 118.6, 118.0, 114.0, 111.7, 111.2, 54.8, 28.0. ESI-HRMS calculated for $C_{24}H_{21}N_3O_3$ [M + H]$^+$: 400.1661. Found: 400.1682.

***N*-(1-Amino-1-oxo-3-phenylpropan-2-yl)-6-(thiophen-2-yl)nicotinamide (34)** was prepared according to method A except using Fmoc-protected phenylalanine (1.3 mmol), 6-bromopyridine-3-carboxylic acid (0.975 mmol), and 2-thiopheneboronic acid (1.3 mmol). Preparative HPLC of the final product followed by lyophilization gave a white powder (>95% purity by analytical HPLC). Yield: 7.5 mg, 6.57%. ^{1}H NMR (400 MHz, DMSO-d_6): δ 2.94 (dd, J = 10.8 Hz, J = 30 Hz, 1H), 3.12 (dd, J = 9.2 Hz, J = 30 Hz, 1H), 4.64 (ddd, J = 8.4 Hz, J = 9.2 Hz, J = 10.8 Hz, 1H), 7.12 (bs, 1H), 7.13−7.34 (m, 6H), 7.58 (bs, 1H), 7.69 (dd, J = 1.2 Hz, J = 4.8 Hz, 1H), 7.87 (dd, J = 1.2 Hz, J = 3.6 Hz, 1H), 7.97 (d, J = 8.1 Hz, 1H), 8.13 (dd, J = 2 Hz, J = 8.4 Hz, 1H), 8.71 (d, J = 8.4 Hz, 1H), 8.83 (d, J = 0.8 1H). ^{13}C NMR (100 MHz, DMSO-d_6): δ 173.6, 164.9, 154.2, 149.1, 144.0, 138.9, 136.6, 130.2, 129.6 (2C), 129.1, 128.5 (2C), 128.1, 127.1, 126.7, 118.4, 55.1, 37.7. ESI-HRMS calculated for $C_{19}H_{17}N_3O_2S$ [M + H]$^+$: 352.1119. Found: 352.1109.

Acknowledgment. We thank Alun Jones, Manager, Mass Spectrometry, Institute for Molecular Bioscience, The Australian Research Council Special Research Centre for Functional and Applied Genomics, and the Cooperative Research Centre for Chronic Inflammatory Disease for equipment access. This work was supported by Australian National Health and Medical Research Council Project Grant 455949 and the Australian Research Council.

Supporting Information Available: Additional experimental procedures and analytical data. This material is available free of charge via the Internet at http://pubs.acs.org.

References

(1) Simmons, D. L.; Botting, R. M.; Hla, T. Cyclooxygenase isozymes: the biology of prostaglandin synthesis and inhibition. *Pharmacol. Rev*. **2004**, *56*, 387–437.
(2) Helliwell, R. J.; Adams, L. F.; Mitchell, M. D. Prostaglandin synthases: recent developments and a novel hypothesis. *Prostaglandins, Leukotrienes Essent. Fatty Acids* **2004**, *70*, 101–113.
(3) Sugimoto, Y.; Narumiya, S. Prostaglandin E receptors. *J. Biol. Chem*. **2007**, *282*, 11613–11617.
(4) Pettipher, R.; Hansel, T. T. Antagonists of the prostaglandin D2 receptor CRTH2. *Drug News Perspect*. **2008**, *21*, 317–322.
(5) FitzGerald, G. A. COX-2 in play at the AHA and the FDA. *Trends Pharmacol. Sci*. **2007**, *28*, 303–307.
(6) Francois, H.; Athirakul, K.; Howell, D.; Dash, R.; Mao, L.; Kim, H. S.; Rockman, H. A.; Fitzgerald, G. A.; Koller, B. H.; Coffman, T. M. Prostacyclin protects against elevated blood pressure and cardiac fibrosis. *Cell Metab*. **2005**, *2*, 201–207.
(7) Arimura, A.; Yasui, K.; Kishino, J.; Asanuma, F.; Hasegawa, H.; Kakudo, S.; Ohtani, M.; Arita, H. Prevention of allergic inflammation by a novel prostaglandin receptor antagonist, S-5751. *J. Pharmacol. Exp. Ther*. **2001**, *298*, 411–419.
(8) Matsuoka, T.; Hirata, M.; Tanaka, H.; Takahashi, Y.; Murata, T.; Kabashima, K.; Sugimoto, Y.; Kobayashi, T.; Ushikubi, F.; Aze, Y.; Eguchi, N.; Urade, Y.; Yoshida, N.; Kimura, K.; Mizoguchi, A.; Honda, Y.; Nagai, H.; Narumiya, S. Prostaglandin D2 as a mediator of allergic asthma. *Science* **2000**, *287*, 2013–2017.
(9) Fujitani, Y.; Kanaoka, Y.; Aritake, K.; Uodome, N.; Okazaki-Hatake, K.; Urade, Y. Pronounced eosinophilic lung inflammation

and Th2 cytokine release in human lipocalin-type prostaglandin D synthase transgenic mice. *J. Immunol.* **2002**, *168*, 443–449.
(10) Mohri, I.; Taniike, M.; Taniguchi, H.; Kanekiyo, T.; Aritake, K.; Inui, T.; Fukumoto, N.; Eguchi, N.; Kushi, A.; Sasai, H.; Kanaoka, Y.; Ozono, K.; Narumiya, S.; Suzuki, K.; Urade, Y. Prostaglandin D2-mediated microglia/astrocyte interaction enhances astrogliosis and demyelination in twitcher. *J. Neurosci.* **2006**, *26*, 4383–4393.
(11) Trivedi, S. G.; Newson, J.; Rajakariar, R.; Jacques, T. S.; Hannon, R.; Kanaoka, Y.; Eguchi, N.; Colville-Nash, P.; Gilroy, D. W. Essential role for hematopoietic prostaglandin D2 synthase in the control of delayed type hypersensitivity. *Proc. Natl. Acad. Sci. U.S.A.* **2006**, *103*, 5179–5184.
(12) Kanaoka, Y.; Urade, Y. Hematopoietic prostaglandin D synthase. *Prostaglandins, Leukotrienes Essent. Fatty Acids* **2003**, *69*, 163–167.
(13) Urade, Y.; Hayaishi, O. Biochemical, structural, genetic, physiological, and pathophysiological features of lipocalin-type prostaglandin D synthase. *Biochim. Biophys. Acta* **2000**, *1482*, 259–271.
(14) Ji, X.; von Rosenvinge, E. C.; Johnson, W. W.; Tomarev, S. I.; Piatigorsky, J.; Armstrong, R. N.; Gilliland, G. L. Three-dimensional structure, catalytic properties, and evolution of a sigma class glutathione transferase from squid, a progenitor of the lens *S*-crystallins of cephalopods. *Biochemistry* **1995**, *34*, 5317–5328.
(15) Thomson, A. M.; Meyer, D. J.; Hayes, J. D. Sequence, catalytic properties and expression of chicken glutathione-dependent prostaglandin D2 synthase, a novel class sigma glutathione *S*-transferase. *Biochem. J.* **1998**, *333*, 317–325.
(16) Tomarev, S. I.; Zinovieva, R. D.; Guo, K.; Piatigorsky, J. Squid glutathione *S*-transferase. Relationships with other glutathione *S*-transferases and *S*-crystallins of cephalopods. *J. Biol. Chem.* **1993**, *268*, 4534–4542.
(17) Sommer, A.; Rickert, R.; Fischer, P.; Steinhart, H.; Walter, R. D.; Liebau, E. A dominant role for extracellular glutathione *S*-transferase from *Onchocerca volvulus* is the production of prostaglandin D2. *Infect. Immun.* **2003**, *71*, 3603–3606.
(18) Jowsey, I. R.; Thomson, A. M.; Flanagan, J. U.; Murdock, P. R.; Moore, G. B.; Meyer, D. J.; Murphy, G. J.; Smith, S. A.; Hayes, J. D. Mammalian class sigma glutathione *S*-transferases: catalytic properties and tissue-specific expression of human and rat GSH-dependent prostaglandin D2 synthases. *Biochem. J.* **2001**, *359*, 507–516.
(19) Hayes, J. D.; Flanagan, J. U.; Jowsey, I. R. Glutathione transferases. *Annu. Rev. Pharmacol. Toxicol.* **2005**, *45*, 51–88.
(20) Oakley, A. J. Glutathione transferases: new functions. *Curr. Opin. Struct. Biol.* **2005**, *15*, 716–723.
(21) Kanaoka, Y.; Ago, H.; Inagaki, E.; Nanayama, T.; Miyano, M.; Kikuno, R.; Fujii, Y.; Eguchi, N.; Toh, H.; Urade, Y.; Hayaishi, O. Cloning and crystal structure of hematopoietic prostaglandin D synthase. *Cell* **1997**, *90*, 1085–1095.
(22) Pinzar, E.; Miyano, M.; Kanaoka, Y.; Urade, Y.; Hayaishi, O. Structural basis of hematopoietic prostaglandin D synthase activity elucidated by site-directed mutagenesis. *J. Biol. Chem.* **2000**, *275*, 31239–31244.
(23) Aritake, K.; Kado, Y.; Inoue, T.; Miyano, M.; Urade, Y. Structural and functional characterization of HQL-79, an orally selective inhibitor of human hematopoietic prostaglandin D synthase. *J. Biol. Chem.* **2006**, *281*, 15277–15286.
(24) Matsushita, N.; Aritake, K.; Takada, A.; Hizue, M.; Hayashi, K.; Mitsui, K.; Hayashi, M.; Hirotsu, I.; Kimura, Y.; Tani, T.; Nakajima, H. Pharmacological studies on the novel antiallergic drug HQL-79: II. Elucidation of mechanisms for antiallergic and antiasthmatic effects. *Jpn. J. Pharmacol.* **1998**, *78*, 11–22.
(25) Matsushita, N.; Hizue, M.; Aritake, K.; Hayashi, K.; Takada, A.; Mitsui, K.; Hayashi, M.; Hirotsu, I.; Kimura, Y.; Tani, T.; Nakajima, H. Pharmacological studies on the novel antiallergic drug HQL-79: I. Antiallergic and antiasthmatic effects in various experimental models. *Jpn. J. Pharmacol.* **1998**, *78*, 1–10.
(26) Hohwy, M.; Spadola, L.; Lundquist, B.; Hawtin, P.; Dahmen, J.; Groth-Clausen, I.; Nilsson, E.; Persdotter, S.; von Wachenfeldt, K.; Folmer, R. H.; Edman, K. Novel prostaglandin D synthase inhibitors generated by fragment-based drug design. *J. Med. Chem.* **2008**, *51*, 2178–2186.
(27) Weber, J. E.; Oakley, A. J.; Christ, A. N.; Clark, A. G.; Hayes, J. D.; Hall, R.; Hume, D. A.; Board, P. G.; Smythe, M. L.; Flanagan, J. U. Identification and characterisation of new inhibitors for the human hematopoietic prostaglandin D2 synthase. *Eur. J. Med. Chem.* **2010**, *45*, 447–454.
(28) Joo, M.; Kwon, M.; Cho, Y. J.; Hu, N.; Pedchenko, T. V.; Sadikot, R. T.; Blackwell, T. S.; Christman, J. W. Lipopolysaccharide-dependent interaction between PU.1 and c-Jun determines production of lipocalin-type prostaglandin D synthase and prostaglandin D2 in macrophages. *Am. J. Physiol.: Lung Cell. Mol. Physiol.* **2009**, *296*, L771–L779.
(29) Joo, M.; Kwon, M.; Sadikot, R. T.; Kingsley, P. J.; Marnett, L. J.; Blackwell, T. S.; Peebles, R. S., Jr.; Urade, Y.; Christman, J. W. Induction and function of lipocalin prostaglandin D synthase in host immunity. *J. Immunol.* **2007**, *179*, 2565–2575.
(30) Funk, C. D. Prostaglandins and leukotrienes: advances in eicosanoid biology. *Science* **2001**, *294*, 1871–1875.
(31) Lewis, R. A.; Soter, N. A.; Diamond, P. T.; Austen, K. F.; Oates, J. A.; Roberts, L. J., 2nd. Prostaglandin D2 generation after activation of rat and human mast cells with anti-IgE. *J. Immunol.* **1982**, *129*, 1627–1631.
(32) Murray, J. J.; Tonnel, A. B.; Brash, A. R.; Roberts, L. J., 2nd; Gosset, P.; Workman, R.; Capron, A.; Oates, J. A. Release of prostaglandin D2 into human airways during acute antigen challenge. *N. Engl. J. Med.* **1986**, *315*, 800–804.
(33) Naclerio, R. M.; Meier, H. L.; Kagey-Sobotka, A.; Adkinson, N. F., Jr.; Meyers, D. A.; Norman, P. S.; Lichtenstein, L. M. Mediator release after nasal airway challenge with allergen. *Am. Rev. Respir. Dis.* **1983**, *128*, 597–602.
(34) Bochner, B. S.; Charlesworth, E. N.; Lichtenstein, L. M.; Derse, C. P.; Gillis, S.; Dinarello, C. A.; Schleimer, R. P. Interleukin-1 is released at sites of human cutaneous allergic reactions. *J. Allergy Clin. Immunol.* **1990**, *86*, 830–839.
(35) Charlesworth, E. N.; Kagey-Sobotka, A.; Schleimer, R. P.; Norman, P. S.; Lichtenstein, L. M. Prednisone inhibits the appearance of inflammatory mediators and the influx of eosinophils and basophils associated with the cutaneous late-phase response to allergen. *J. Immunol.* **1991**, *146*, 671–676.
(36) Proud, D.; Sweet, J.; Stein, P.; Settipane, R. A.; Kagey-Sobotka, A.; Friedlaender, M. H.; Lichtenstein, L. M. Inflammatory mediator release on conjunctival provocation of allergic subjects with allergen. *J. Allergy Clin. Immunol.* **1990**, *85*, 896–905.
(37) Honda, K.; Arima, M.; Cheng, G.; Taki, S.; Hirata, H.; Eda, F.; Fukushima, F.; Yamaguchi, B.; Hatano, M.; Tokuhisa, T.; Fukuda, T. Prostaglandin D2 reinforces Th2 type inflammatory responses of airways to low-dose antigen through bronchial expression of macrophage-derived chemokine. *J. Exp. Med.* **2003**, *198*, 533–543.
(38) Aikawa, T.; Shimura, S.; Sasaki, H.; Ebina, M.; Takishima, T. Marked goblet cell hyperplasia with mucus accumulation in the airways of patients who died of severe acute asthma attack. *Chest* **1992**, *101*, 916–921.
(39) Inoue, T.; Irikura, D.; Okazaki, N.; Kinugasa, S.; Matsumura, H.; Uodome, N.; Yamamoto, M.; Kumasaka, T.; Miyano, M.; Kai, Y.; Urade, Y. Mechanism of metal activation of human hematopoietic prostaglandin D synthase. *Nat. Struct. Biol.* **2003**, *10*, 291–296.
(40) Shimamoto, S.; Yoshida, T.; Inui, T.; Gohda, K.; Kobayashi, Y.; Fujimori, K.; Tsurumura, T.; Aritake, K.; Urade, Y.; Ohkubo, T. NMR solution structure of lipocalin-type prostaglandin D synthase: evidence for partial overlapping of catalytic pocket and retinoic acid-binding pocket within the central cavity. *J. Biol. Chem.* **2007**, *282*, 31373–31379.
(41) Urade, Y.; Ujihara, M.; Horiguchi, Y.; Igarashi, M.; Nagata, A.; Ikai, K.; Hayaishi, O. Mast cells contain spleen-type prostaglandin D synthetase. *J. Biol. Chem.* **1990**, *265*, 371–375.
(42) Mohri, I.; Aritake, K.; Taniguchi, H.; Sato, Y.; Kamauchi, S.; Nagata, N.; Maruyama, T.; Taniike, M.; Urade, Y. Inhibition of prostaglandin D synthase suppresses muscular necrosis. *Am. J. Pathol.* **2009**, *174*, 1735–1744.
(43) Terada, N.; Yamakoshi, T.; Hasegawa, M.; Tanikawa, H.; Maesako, K.; Ishikawa, K.; Konno, A. The effect of ramatroban (BAY u 3405), a thromboxane A2 receptor antagonist, on nasal cavity volume and minimum cross-sectional area and nasal mucosal hemodynamics after nasal mucosal allergen challenge in patients with perennial allergic rhinitis. *Acta Otolaryngol. Suppl.* **1998**, *537*, 32–37.
(44) Ikai, K.; Ujihara, M.; Fujii, K.; Urade, Y. Inhibitory effect of tranilast on prostaglandin D synthetase. *Biochem. Pharmacol.* **1989**, *38*, 2673–2676.
(45) Horton, D. A.; Bourne, G. T.; Smythe, M. L. The combinatorial synthesis of bicyclic privileged structures or privileged substructures. *Chem. Rev.* **2003**, *103*, 893–930.
(46) Horton, D. A.; Severinsen, R.; Kofod-Hansen, M.; Bourne, G. T.; Smythe, M. L. A versatile synthetic approach to peptidyl privileged structures using a "safety-catch" linker. *J. Comb. Chem.* **2005**, *7*, 421–435.
(47) Severinsen, R.; Bourne, G. T.; Tran, T. T.; Ankersen, M.; Begtrup, M.; Smythe, M. L. Library of biphenyl privileged substructures using a safety-catch linker approach. *J. Comb. Chem.* **2008**, *10*, 557–566.

(48) Funk, C. D.; Fitzgerald, G. A. COX-2 inhibitors and cardiovascular risk. *J. Cardiovasc. Pharmacol.* **2007**, *50*, 470–479.
(49) Bradford, M. M. A rapid and sensitive method for the quantitation of microgram quantities of protein utilizing the principle of protein-dye binding. *Anal. Biochem.* **1976**, *72*, 248–254.
(50) Irvine, K. M.; Andrews, M. R.; Fernandez-Rojo, M. A.; Schroder, K.; Burns, C. J.; Su, S.; Wilks, A. F.; Parton, R. G.; Hume, D. A.; Sweet, M. J. Colony-stimulating factor-1 (CSF-1) delivers a proatherogenic signal to human macrophages. *J. Leukocyte Biol.* **2009**, *85*, 278–288.
(51) Irvine, K. M.; Burns, C. J.; Wilks, A. F.; Su, S.; Hume, D. A.; Sweet, M. J. A CSF-1 receptor kinase inhibitor targets effector functions and inhibits pro-inflammatory cytokine production from murine macrophage populations. *FASEB J.* **2006**, *20*, 1921–1923.